Causal mechanisms in airfoil-circulation formation

J. Y. Zhu, T. S. Liu, L. Q. Liu, S. F. Zou, and J. Z. Wu

Citation: Physics of Fluids **27**, 123601 (2015); doi: 10.1063/1.4937348
View online: https://doi.org/10.1063/1.4937348
View Table of Contents: http://aip.scitation.org/toc/phf/27/12
Published by the American Institute of Physics

PHYSICS OF FLUIDS **27**, 123601 (2015)

Causal mechanisms in airfoil-circulation formation

J. Y. Zhu,[1] T. S. Liu,[2] L. Q. Liu,[1] S. F. Zou,[1] and J. Z. Wu[1,3,a)]
[1]*State Key Laboratory for Turbulence and Complex Systems, College of Engineering, Peking University, Beijing 100871, China*
[2]*Department of Mechanical and Aerospace Engineering, Western Michigan University, Kalamazoo, Michigan 49008, USA*
[3]*The University of Tennessee Space Institute, Tullahoma, Tennessee 37388, USA*

(Received 12 February 2015; accepted 16 November 2015; published online 23 December 2015)

In this paper, we trace the dynamic origin, rather than any kinematic interpretations, of lift in two-dimensional flow to the physical root of airfoil circulation. We show that the key causal process is the vorticity creation by tangent pressure gradient at the airfoil surface via no-slip condition, of which the theoretical basis has been given by Lighthill ["Introduction: Boundary layer theory," in *Laminar Boundary Layers*, edited by L. Rosenhead (Clarendon Press, 1963), pp. 46–113], which we further elaborate. This mechanism can be clearly revealed in terms of vorticity formulation but is hidden in conventional momentum formulation, and hence has long been missing in the history of one's efforts to understand lift. By a careful numerical simulation of the flow around a NACA-0012 airfoil, and using both Eulerian and Lagrangian descriptions, we illustrate the detailed transient process by which the airfoil gains its circulation and demonstrate the dominating role of relevant dynamical causal mechanisms at the boundary. In so doing, we find that the various statements for the establishment of Kutta condition in steady inviscid flow actually correspond to a sequence of events in unsteady viscous flow. [http://dx.doi.org/10.1063/1.4937348]

I. INTRODUCTION

The first cornerstone of modern aerodynamics, and also the simplest and one of the most important force formulae in the entire fluid dynamics, is the famous lift formula

$$L = -\rho U\Gamma, \quad \Gamma = \oint_C \boldsymbol{u}\cdot\boldsymbol{t}dl = \int_S \omega dS, \tag{1}$$

originally established by Kutta[1] and Joukowski[2] for an airfoil in incompressible and irrotational 2D steady flow. Here, ρ and U are the constant density and velocity of the uniform incoming flow, C is a properly chosen contour surrounding the airfoil with unit tangent vector $\boldsymbol{t}$, and S is the area spanned by C. $\Gamma > 0$ if counted counterclockwise. Along with the Kutta condition imposed at the sharp trailing edge (TE), this Kutta-Joukowski formula has served as the very basis of classic steady aerodynamics.

In sharp contrast to the great simplicity of the lift-circulation relationship revealed by (1) is the long history of one's efforts in clarifying the physical root of airfoil circulation.[3–5] This issue has been persisted for more than a century and remained interesting, due to its fundamental importance in optimal wing design and flow controls. However, so far a complete interpretation of the origin of lift has not yet been widely available.

The main objective of the present paper is to make up a long-time missing piece of the story. To explain our goal, we first briefly recall some events in the history of one's understanding of the physics behind (1).

In potential-flow theory from which (1) was originally derived, the airfoil circulation had nowhere to be identified but could only be idealized as being "induced" by a point vortex inside the airfoil,

a)Electronic mail: jzwu@coe.pku.edu.cn

which is not a real physical entity. It was Prandtl's boundary-layer theory that revealed the viscous origin of (1) and indicated that *the true physical carrier of airfoil's circulation is its boundary layers.* Indeed, the correctness of (1) in viscous flow has been confirmed by Bryant *et al.*[6] and Taylor,[7] among others, both experimentally and theoretically. Since in this case the contour C for computing Γ must cut the viscous wake, Taylor[7] pointed out that the segment of C in the wake must be perpendicular to the direction of incoming flow to avoid that the viscous profile drag has any effect on lift. He then proved that with this choice the net vorticity flux through the segment of C in wake is zero, and hence Γ is independent of the contour size. But Taylor's proof of (1) for viscous flow is not without flaw; a remedy has been given by Liu *et al.*[5]

The viscous origin of circulation has also been confirmed, though less directly, by Prandtl's success in extending (1) to the 3D lift problem, known as lifting-line theory. Since then low-speed aerodynamics was quickly established in which, as stressed by Glauert[8] and von Kármán and Burgers,[9] the apparently "inviscid" flow is actually treated as the asymptotic limit of $Re \to \infty$, or with viscosity $\mu \neq 0$ but $\mu \to 0$. Then, the carrier of vorticity and circulation is the infinitely thin attached and free *vortex sheets* generated by the wing.

To further enhance one's understanding of the origin of lift, it is necessary to interpret in detail the formation process of circulation by typical case studies. Starting flow over airfoil, either impulsively or by acceleration, is such a case. Thus, Prandtl and Tietjens[10] gave a sketch of the streamline pattern over an airfoil in the first instant of motion. They demonstrated the existence of airfoil circulation by the experimentally observed starting vortex and total-circulation conservation theorem (cf. Liu *et al.*[5]). von Kármán and Burgers[9] and Batchelor[11] also discussed the circulation-formation process. Batchelor's qualitative interpretation is so far in most detail. It clearly indicates that the formation of circulation involves a complex chain of mechanisms or multiple events and can be summarized as follows. The initial motion is an irrotational flow, and the fluid moves around the sharp TE from the lower surface to the upper surface, leading to an extremely low pressure at TE. Due to the viscosity and adverse pressure gradient, a back flow appears on the upper surface very close to TE, making the original flow separate from the airfoil surface, and produce a starting vortex. As the starting vortex separates from the airfoil, a circulation of the same magnitude but opposite sign is left around the airfoil. That is, the airfoil acquires the initial circulation. In the final steady motion, the circulation prescribed by Kutta condition is the only possible value for the airfoil.

On the other hand, a few numerical simulations have been performed to quantitatively study the circulation-formation process, including identifying some of the chain events.[12–15] For example, Lugt and Haussling[12] gave a detailed time evolution of streamlines for laminar flow past an abruptly accelerated elliptic cylinder at 45° incidence, as well as the time of the establishment of Kutta condition at Reynolds number $Re = 200$ based on the focal distance of ellipse. Recently, one's interest on circulation has been mainly focused on separated flows with leading-edge vortex.[16,17] Remarkably, Tam[18] has found that the wing flexibility may cause more vorticity to shed at a turning point and hence create additional lift.

Thus far one's seek for the origin of lift has been correctly locked to the viscous carrier of the airfoil circulation, provided by the vorticity (more specifically, by the Lamb vector) in airfoil's boundary layers. The initial appearance of starting vortex has been widely considered as the proof of the existence of the airfoil circulation. However, this scenario is not yet a complete story. In this regard, we agree with McLean,[19] who stressed the crucial importance of identifying the *cause-and-effect mechanisms* in the whole process of lift generation. Indeed, McLean has used this causality criterion to easily disqualify many misconceptions about the origin of lift that are popular among those readers outside fluid physics. McLean also commented on the Kutta-Joukowski theorem (p. 299): *"its general progression does not reflect physical cause and effect"; "The starting vortex and the circulation are actually more properly seen as byproducts of the lift than as causes."*

Of course, the boundary-layer theory has revealed some of the causal mechanisms in the formation of lift, such as the advection and diffusion of vortical flow in the layer caused by streamwise pressure gradient and diffusion, respectively. However, due to the reason to be explained in Sec. II, conventionally formulated boundary-layer theory in terms of momentum consideration can only tell the inevitable *existence* of this viscous and rotational layer adjacent to the wall, but the very first causal mechanism in the whole chain of events is the *vorticity generation at the wall*. Although at Prandtl's

time it must have been recognized that vorticity is generated at the airfoil surface via viscosity and no-slip condition, the *local quantitative dynamic theory* of this key mechanism is still lacking.

Actually, the desired theory has been provided by Lighthill,[20] who revealed that the vorticity creation at a stationary solid wall is caused by tangent pressure gradient via no-slip condition. Surprisingly, the theory has existed for half-century but never been applied to the study of the origin of lift. Thus, what we need to do first here is simply elaborating Lighthill's theory and identifying the relevant causal mechanisms. We then apply the theory to our careful numerical simulation of 2D starting flow over airfoil to gain a thorough understanding of the chain of events in circulation formation, with emphasis on the causality therein.

As an interesting byproduct of our study, we also examine the specific events at which the Kutta condition, originally imposed to steady inviscid flow, is naturally realized in viscous flow. We find that various statements of the Kutta condition by different authors, though merging to a single one in the final steady state, are realized at different times in the transient starting flow. This finding may be of interest in developing unsteady Kutta condition.

In Section II, we review Lighthill's theory that permits tracing the origin of circulation to the very root of vorticity generation and identify the cause and effect therein. In Section III, we present our Navier-Stokes simulation of starting flow over an airfoil, display the flow-pattern evolution history, and identify the causal mechanisms during the whole transient process. In Section IV, we examine the respective realizations of the Kutta condition stated in different ways for steady inviscid flow. Conclusions are made in Section V.

II. CAUSAL MECHANISMS OF VORTICITY CREATION AT BOUNDARY

A. Lighthill's relations

Consider a two-dimensional unsteady flow over a stationary airfoil. We start from the component form of the Navier-Stokes equation in instantaneous streamline coordinates (n, s), see Fig. 1. There, $\boldsymbol{t}$ and $\boldsymbol{n}$ are the unit tangent and normal vectors of any streamline (including the airfoil ∂B) such that $\boldsymbol{u} = \boldsymbol{t}q$, and $\boldsymbol{t}$ is assumed to move counterclockwise viewed on the fluid side, so that $(\boldsymbol{n}, \boldsymbol{t}, \boldsymbol{e}_z)$ form a right-hand orthonormal triad. Then, the Navier-Stokes equation yields

$$\frac{1}{\rho}\frac{\partial p}{\partial s} = -\frac{\partial q}{\partial t} - q\frac{\partial q}{\partial s} + \nu\frac{\partial \omega}{\partial n} - q\frac{\partial \boldsymbol{t}}{\partial t}\cdot\boldsymbol{t}, \tag{2a}$$

$$\frac{1}{\rho}\frac{\partial p}{\partial n} = -\kappa q^2 - \nu\frac{\partial \omega}{\partial s} - q\frac{\partial \boldsymbol{t}}{\partial t}\cdot\boldsymbol{n}, \tag{2b}$$

where κ is the curvature of streamline.

We now apply (2) directly to airfoil surface ∂B. By *acceleration adherence* $D\boldsymbol{u}/Dt = \boldsymbol{0}$ at ∂B, which is a corollary of velocity adherence, we obtain a pair of on-wall relations

$$\frac{1}{\rho}\frac{\partial p}{\partial s} = \nu\frac{\partial \omega}{\partial n} \equiv \sigma, \tag{3a}$$

$$\frac{1}{\rho}\frac{\partial p}{\partial n} = -\nu\frac{\partial \omega}{\partial s}, \tag{3b}$$

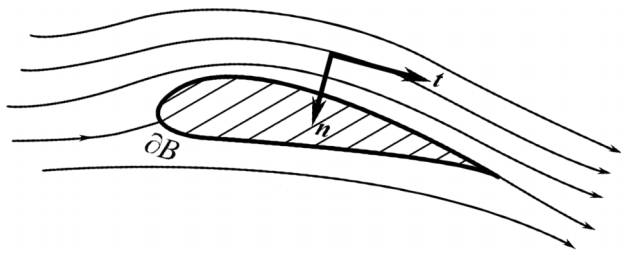

FIG. 1. Two-dimensional steady streamlines over an airfoil and intrinsic coordinates.

which will be referred to as *Lighthill's relations*. Here, (3a) is the kernel result of Lighthill,[20] who identified the normal diffusion flux of vorticity as the measure of vorticity creation rate at the wall, which we call the boundary vorticity flux (BVF). Thus, (3a) implies that on a stationary wall tangent pressure gradient can *produce vorticity from none* at the wall via acceleration no-slip condition. The created vorticity is then diffused into the fluid. This is the desired local dynamic causal mechanism. Note that since generically tangent pressure gradient is of $O(1)$, so must be BVF. Thus, as $Re \to \infty$, there must be $\partial_n \omega \to O(Re)$.

It will be seen in Section III D that the boundary (σ, ω)-coupling reflected by Lighthill's relations plays an important role for fully understanding the establishment of the airfoil circulation in starting flow. More generally, these relations can be easily generalized to three-dimensional and unsteady flow over arbitrarily moving/deforming bodies with external body force, as well as to compressible flow.[21] But the core causal mechanisms remain the same as addressed above. Actually, the general significance of (3a) in optimal configuration design and on-wall flow control has been demonstrated by several engineering applications as reviewed by Wu *et al.*[22] As another recent example, Zhu *et al.*[23] have demonstrated that an airfoil with "effective slip boundary" may enjoy a super lift/drag ratio at large angles of attack without boundary-layer separation, of which the underlying physics is nothing but *BVF-based flow control* that can alter the boundary-layer formation as one desires.

B. Causal mechanisms in vorticity creation and boundary-layer formation

More specifically, when a body moves in a general compressible viscous fluid (where p should be understood as modified by a viscous dilatation term), it produces normal stress p as the first causal mechanism since pressure is a result of molecular collisions in equilibrium state. This is an inviscid process with time scale $t_p \sim c/a$, where c is the characteristic length scale of the body (e.g., chord length for an airfoil), and a is the speed of sound. In the present incompressible flow $t_p \to 0$. The appearance of viscous shear stress $\tau = -\mu\omega$ at the wall comes after a short relaxation time (a few collisions of molecules),[24] and the on-wall vorticity starts to diffuse immediately. Thus, strictly, tangent pressure gradient causes BVF, but they occur almost simultaneously since the relaxation time can be neglected in the local equilibrium assumption used throughout the continuous fluid dynamics.

Then, once the vorticity generated at the wall enters the fluid, it is both advected downstream by tangent pressure gradient and diffused across the flow by normal vorticity gradient. The advection time scale is $t_a \sim c/U$ so that $t_p/t_a = M$ with M being the Mach number. The diffusion time scale, say t_ω, comes from the balance of terms in linear diffusion equation,

$$\frac{\partial \omega}{\partial t} \sim \nu \frac{\partial^2 \omega}{\partial n^2},$$

so there is $t_\omega = \delta^2/\nu$ where δ is the effective normal diffusion distance. Thus, during the advection time t_a by which a fluid particle travels the chord length c, the newly created vorticity will be diffused along the normal to a distance

$$\delta_c \sim \sqrt{\nu t_a} = c Re_c^{-1/2}, \quad Re_c = Uc/\nu. \tag{4}$$

This δ_c measures the thickness of the near-wall vortical-flow region, which at $Re \gg 1$ is the boundary layer. This observation reveals that *a boundary layer (including boundary vorticity, denoted by ω_B) is an accumulated effect of vorticity creation, diffusion, and advection in both space and time.* In this way, the circulation is gradually established, since it is the domain integral of vorticity.

Compared to (3a), (3b) implies a balance of normal pressure gradient (NPG) and tangent diffusion flux of existing ω_B. Its role is much less significant at large Reynolds number, since tangent diffusion flux of vorticity is generically of $O(Re^{-1/2})$, and hence so must be normal pressure gradient, in agreement with the boundary-layer theory. Besides, no new vorticity creation is involved in (3b). However, to examine the flow behavior near the sharp TE, it is advantageous to apply (2b) not to ∂B but to streamlines sufficiently close to ∂B, say within a sublayer of the boundary layer adjacent to the wall, where the orientation of $\boldsymbol{t}$ is aligned to ∂B and nearly time-independent (except isolated separation and/or attachment points). Then, there is

$$\frac{1}{\rho}\frac{\partial p}{\partial n} = -\kappa q^2 - \nu\frac{\partial \omega}{\partial s} \quad \text{very close to } \partial B. \tag{5}$$

Unlike (3b), here the normal pressure gradient is mainly balanced by κq^2. When the flow does not separate at TE, slightly away from TE there is very rapid flow turning around it. Since $\kappa \gg 0$ there by our chosen triad $(\boldsymbol{n},\boldsymbol{t},\boldsymbol{e}_z)$, this implies very strong negative peak of normal pressure gradient. As we shall see in Section III C, this big suction peak at TE is a dynamic cause with very strong effect on the flow evolution.

We may further define the *boundary enstrophy flux* by[21]

$$\eta \equiv \nu\frac{\partial}{\partial n}\left(\frac{1}{2}\omega^2\right) = \boldsymbol{\omega}_B \cdot \boldsymbol{\sigma} = \frac{\omega}{\rho}\frac{\partial p}{\partial s}, \tag{6}$$

which is a simple marker of the dynamic interaction between BVF and ω_B. $\eta > 0$ implies that the newly produced vorticity by BVF is of the same sign as the existing one and to enhance it, like the case of favorable pressure gradient in a boundary layer that ensures the attachment of the layer. $\eta < 0$ implies that the newly produced vorticity is weakening the existing one, implying that flow separation is about to happen.

C. Momentum formulation vs vorticity formulation

We remark that Lighthill's relation (3a) is not an organic ingredient of the conventional *momentum formulation* in terms of primitive variables $(\boldsymbol{u},p)$. There, a well-posed problem consists of continuity equation $\nabla\cdot\boldsymbol{u} = 0$ and momentum equation (2) along with velocity adherence, and (3a) is just a natural on-wall result that any $(\boldsymbol{u},p)$-solution should satisfy. In fact, in boundary-layer approximation, a condition equivalent to (3a) has been observed and called a *compatibility condition* (Schlichting and Gersten,[25] p. 166),

$$\mu\left(\frac{\partial^2 u}{\partial y^2}\right)_w = \frac{dp}{dx},$$

which however plays no further role in theoretical development.

In contrast to the momentum formulation, (3a) is an explicit and inherent component of the *vorticity formulation*, pioneered in the same article of Lighthill.[20] There, the governing equation is the curl of (2), namely, vorticity transport equation, which is one order higher than (2). Only velocity adherence is insufficient, since possible spurious solution could appear. Additional boundary condition is necessary; then, a natural choice is acceleration adherence, of which (3a) is a special case on stationary wall. The interior $(\boldsymbol{u},p)$-coupling in the momentum formulation now becomes a *viscous boundary* (σ,ω)-*coupling*. In this way, the mechanism of vorticity generation is an obviously inevitable issue to be fully explored. This could be why Lighthill[20] asserts that *"although momentum considerations suffice to explain the local behavior in a boundary layer, vorticity considerations are needed to place the boundary layer correctly in the flow as a whole."* But how a vorticity boundary condition of Neumann type like (3a) can be numerically implemented is another issue, which will be briefly discussed in Section III B.

It should be stressed that both momentum formulation and vorticity formulation, once well-posed, can of course equally capture the entire physical processes from vorticity creation at the wall as well as its advection and diffusion in boundary layers. But it is of interest to observe that, as the boundary condition of vorticity formulation, (3a) is derived from momentum formulation. Being the vorticity boundary condition, it is redundant in momentum formulation; while being derived from momentum equation, it is not seen either in vorticity formulation if one's attention is merely focused on the vorticity equation itself — this was indeed the case in more than 100 years from the time of Euler, Lagrange, and D'Alembert to the late 19th century, when most masters of each time tried to find the origin of vorticity but failed as reviewed in detail by Truesdell.[26] Even in the early 1950s, Truesdell still wrote with regret, *"more surprising, that the generation of vorticity in viscous fluids is still not well understood, is evidenced by incomplete treatments given in text-books and treatises and by recent papers essentially repeating the errors of prior authors."* This observation could explain the late appearance of Lighthill's theory, almost 60 years after the pioneering works of Kutta, Joukowski,

and Prandtl, and the late recognition of its role in understanding the origin of lift as we do now, another half-century after its appearance.

III. A NUMERICAL STUDY OF FORMATION OF AIRFOIL CIRCULATION IN STARTING FLOW

We now revisit the formation process of airfoil circulation in a starting flow based on our two-dimensional numerical investigation.

A. On the choice of starting-flow mode

One of the important issues in numerical simulation is to specify the time history of starting flow, since different choices of starting-flow profiles have very critical effects on the following flow evolution. It is well known that Prandtl and Tietjens[10] present their experiments for visualizing the formation of starting vortex behind an impulsively started airfoil and use them to confirm the existence of airfoil circulation via the total-circulation conservation theorem. Since then most relevant interpretations of the airfoil-circulation establishment as reviewed in Section I have been based on this impulsive-motion mode, which however covers up some key transient flow phenomena due to the appearance of singularity. Then, at the opposite extreme of impulsively started flow is the actual take-off process, where an aircraft first accelerates on the runway to a sufficiently large finite speed at almost zero angle of attack, and then turns its nose up to gain a lift. How the flow pattern evolves in this smooth and graduate mode has been studied by us using a numerical simulation that mimics the take-off mode of a NACA-0012 airfoil. The angle of attack is assumed to vary according to $\alpha = \alpha_0(t - \sin(\pi t)/\pi)$ for $t < 1$ and $\alpha = \alpha_0 \sin(\pi t/2)$ for $t < 1$, etc. We found that the result is totally different (details not shown here): the starting vortex and its associated complex formation processes can hardly be seen. Thus, this mode is not a good model either to reveal the physical root of lift.

To explore the initial formation of circulation but avoid the strong initial singularity, therefore, in our numerical simulation we assume a gradual acceleration at a constant angle of attack, which somewhat mimics the mode in wind-tunnel experiment. The major event in the formation process is unsteady separation, and the underlying physics will be analyzed in detail in terms of vorticity formulation. The result is consistent with Batchelor's general analysis mentioned in Section I, but with much clearer refined causal mechanisms.

B. Numerical method and validation

We consider a laminar, accelerating uniform incoming flow of incompressible fluid,

$$U_\infty(t) = \begin{cases} \sin(\pi t/2) & \text{if } t < 1.0 \\ 1.0 & \text{if } t \geq 1.0 \end{cases} \tag{7}$$

over a NACA-0012 airfoil at angle of attack $\alpha = 6°$. Flow quantities are made dimensionless by fluid density ρ, airfoil's chord length c, and final incoming velocity $U_\infty = 1$. The Reynolds number $Re(t) = U_\infty(t)c/\nu$ varies as t, and for $0 < t \leq 1.0$ there is $Re(t) = \sin(\pi t/2) \times 10^5$. Note that (7) is only one specific type of starting flow with constant α, and other assumed types will lead to different histories of vorticity flux from surface, but they should possess the same key events to be identified in Subsections III C and III D.

The Navier-Stokes solver we adopted is a vorticity-stream function (ω-ψ) scheme in terms of vorticity formulation. As is well known, the main issue of various vorticity-based schemes is how to prescribe the vorticity boundary condition (ω-BC for short). Since the velocity is related to vorticity through the Biot-Savart law or Poisson equations, the velocity no-slip at boundary imposes an integral *kinematic* constraint to the global vorticity distribution rather than any local ω-BC of *Dirichlet type*. What one can do on the boundary, say $\psi(s) = 0$ with (s,n) being coordinates along and normal to the wall, is to either simply express the boundary vorticity ω_B by $\omega_B \approx u_h/h$ where h is the height of the first mesh above the wall and u_h is the tangent velocity there,[27] or more routinely to relate ω_B and ψ by $\omega_B = -\partial^2\psi/\partial n^2$ and solve the Poisson equation for ψ and vorticity transport equation simultaneously. Then, (3a) can be used to calculate the on-wall pressure distribution (e.g., Chung[28]).

Equation (3a) itself, however, can just be cast to a localized *dynamic* ω-BC of *Neumann type*, if the tangent gradient of unknown pressure can be bypassed. That this is feasible was first argued by Lighthill[20] who conceived a fractional-step method where the convection and diffusion of vorticity are computed successively within each time step Δt. Indeed, due to the linearity of the Poisson equation for p, it can be split to an inviscid convective pressure and a Stokes pressure (the pressure in Stokes flows), say p_i and p_s, respectively, where only the latter has inevitable boundary coupling with ω which makes the ω-BC global. But the decoupling of ω and p_i by no means implies that p_i has no effect on the BVF; rather, in vorticity-based formulation, its effect is fully reflected by a slip velocity u_s or attached vortex sheet $\gamma = -u_s$ "induced" by the entire vorticity field. Then, the no-slip condition turns the vortex sheet to newly produced vorticity. While at small Reynolds numbers p_s is dominant, the situation is opposite at large Reynolds numbers: Wu *et al.*[29] have given theoretical proof and numerical demonstration that in computing the BVF, neglecting its coupling with p_s only causes an error of $O(Re^{-1/2})$. Therefore, a local Neumann condition for the vorticity with good accuracy does exist at sufficiently large Reynolds numbers.

While both approaches (ω-BC of ω_B as Dirichlet type and BVF as Neumann type) may yield high-accuracy results, the preceding discussion in Section II has indicated that the fractional-step method with BVF-based BC is physically more appealing. This approach leads to an approximate BVF at the end of diffusion substep,

$$\nu \frac{\partial \omega}{\partial n} \approx -\frac{u_s}{\Delta t}, \tag{8}$$

which is of $O(1)$ with error of $O(Re^{-1/2})$. Equation (8) is the common form in all vorticity based schemes with dynamic Neumann-type ω-BC.[29–32] It behaves great for computing flows at large Reynolds numbers if Δt is sufficiently small.

The fractional-step scheme we used here was constructed by Zhu[33] for computing airfoil flow, developed from a code of Wu *et al.*[29] who computed impulsively started circular-cylinder flow with the result in excellent agreement with a benchmark experiment and with the high-resolution simulation of Koumoutsakos and Leonard.[32] For computing airfoil flow, Zhu resolved two major numerical difficulties successfully. First, the total vorticity (circulation) cannot be automatically satisfied by the approximate BVF-based BC. It does not matter for a symmetric geometry without rotation such as circular cylinder, but it is of crucial importance for airfoil-flow computations. Zhu[33] found that the simplest and most effective way to ensure the total-circulation conservation at every time step is to add a point vortex inside the airfoil (at the center of transformed unit circle) to induce a small slip velocity Δu_s. Theoretically, the conservation of total-circulation Γ in computational domain is equivalent to the constraint

$$\oint_{\partial B} \sigma ds = 0, \tag{9}$$

which now reads

$$\oint_{\partial B} (u_s + \Delta u_s) = 0. \tag{10}$$

To avoid singularity, the velocity at the trailing edge is always set zero. This is feasible since the velocity there is not to be computed; at most the scheme can obtain the velocities (and pressures) at points U and L closest to the trailing edge at upper and lower surfaces, see Fig. 2.

Second, to ensure accurate resolution of the flow near the trailing edge, Zhu designed a higher quality C-type grid and used an extended conformal mapping to guarantee the grid be orthogonal. Then, by splitting the domain to a front zone and wake zone (Fig. 3), Zhu was able to construct an innovative Poisson solver employing cyclic reduction and over-relaxing Gaussian iteration to solve the Poisson equation $\nabla^2 \psi = -\omega$.

In this code, the convection substep is computed by a second-order TVD Runge-Kutta scheme and the convection term is discretized by QUICK scheme. The diffusion equation is solved by alternating direction implicit (ADI) method which is of second order in both space and time. Zhu[33] has tested a great number of cases to verify the reliability and robustness of the code.

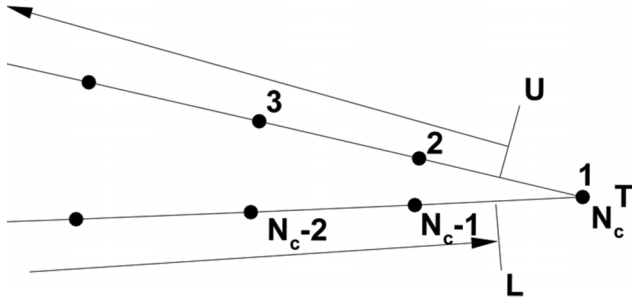

FIG. 2. The illustration of the segmentation integral near the trailing edge. T is the trailing edge point which has two labels 1 and N_c, U is the midpoint between 1 and 2, and L is the midpoint between $N_c - 1$ and N_c.

The test of mesh size and time step size for the current starting flow indicates that denser mesh (at least 600×129 in circumferential and normal directions, respectively) is required (Fig. 4). Thus, in our computation, the mesh distribution is 800×257, where 400 meshes are placed on the airfoil surface and the grid is clustered near the trailing edge. The adopted time step size is $\Delta t = 10^{-4}$.

C. Formation of circulation: Flow patterns

Existing interpretations and numerical studies of circulation formation in starting flow were all confined to Eulerian description and almost solely based on instantaneous streamlines. But since the circulation formation process is a highly unsteady transient process that involves unsteady flow separation, the Eulerian description and separation criterion in terms of instantaneous streamlines are not adequate. As stressed by Kurosaka and Sundaram[34] and Sundaram *et al*.,[35] the appropriate interpretation of unsteady flow pattern should jointly use streaklines and pathlines. Thus, in our study, we use both Eulerian and Lagrangian descriptions, by examining streamlines, pathlines, and streaklines simultaneously. This approach has proved effective to provide much clearer understanding of the evolution of flow pattern.

Pathlines are used to exhibit unsteady separation, which is essentially a Lagrangian process. Streaklines, if particles are continuously released from narrow layers of high vorticity, visualize material shear-layer evolution. The initial and terminal points of the trajectory of a particle labeled by

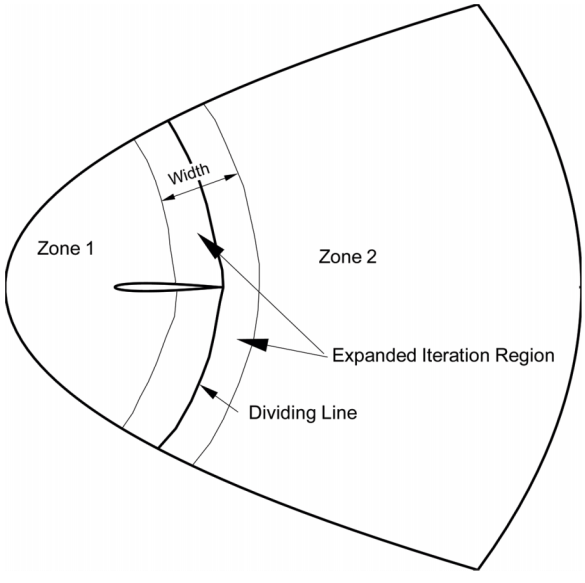

FIG. 3. Two zones in favor of the fast Poisson solver.

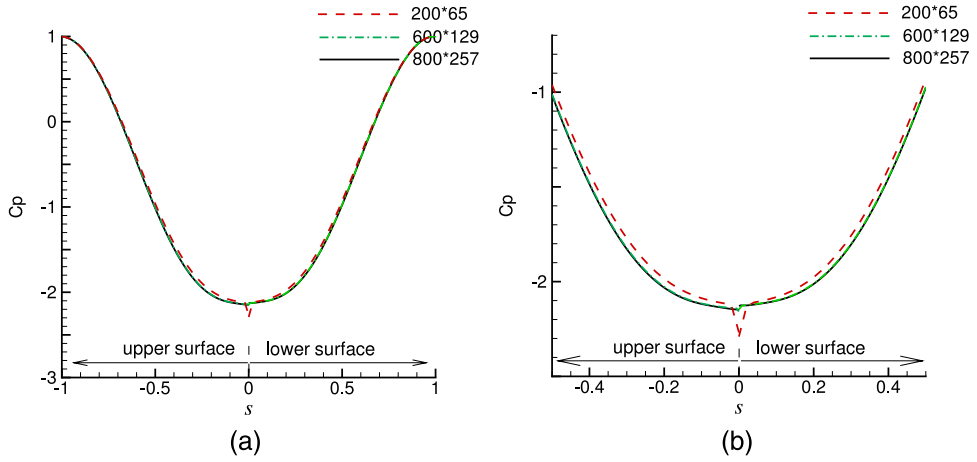

FIG. 4. Tests of mesh dependence: Distribution of pressure coefficient C_p over NACA-0012 airfoil in accelerating incoming flow (7) at $t = 0.03$ with $Re(t) \approx 4711$ and $\alpha = 6°$. (a) Global view; (b) local view near trailing edge. Coordinate s moves around the airfoil surface in clockwise direction, starting from and ending at the leading edge ($-1 \le s \le 1$). $s = 0$ is at trailing edge and $s = \pm 1$ are at leading edge. In (a) and (b), the two closest points at upper and lower surfaces are U and L shown in Fig. 2.

$\boldsymbol{\xi} = \boldsymbol{x}(t_0)$ in a period $t_0 \le t \le t_1$, say, must be the terminal and initial points, respectively, of the streakline formed by a sequence of particles releasing at $\boldsymbol{x}(t_0)$ in the same period. Thus, this pair of pathline and streakline meets at the two endpoints but may diverse in the middle.

Although streamline pattern alone cannot exhibit unsteady separation, we may study the instantaneous topological behavior of vector field $\boldsymbol{u}(\boldsymbol{x}, t)$ in terms of the index rule of its fixed points.[36] Denote node and saddle in V_f by N and S, and semi-node and semi-saddle on ∂B by N' and S', respectively. Recall that the front stagnation point (not shown) is a semi-saddle S', and their total number (denoted by $\sum$) for two-dimensional airfoil flow obeys the rule[21]

$$\left(\sum_{N} + \frac{1}{2}\sum_{N'}\right) - \left(\sum_{S} + \frac{1}{2}\sum_{S'}\right) = -1 \quad \text{at all time.}$$

The computed flow-pattern evolution is shown in Fig. 5 (only parts of flow field near trailing edge are displayed), by which we can examine the time evolution of the flow patterns in detail.

After the airfoil gains a nonzero incoming velocity, the flow pattern at $t = 0.002$ (Fig. 5(a)) is very similar to the corresponding inviscid potential flow, where some fluid particles away from but very close to lower surface turn rapidly around the trailing edge, where as mentioned in Section II B the streamline curvature has become finite, and move upstream. Thus, in addition to the front stagnation point at the airfoil's leading edge, there is a rear semi-saddle point S_1' on its upper surface, which in unsteady flow cannot be identified as separation point.

At $t = 0.02$, a segment of thin sublayer with $\omega < 0$ appears underneath the upper-surface boundary layer (Figs. 5(b) and 5(c)), forming an attached bubble as shown by instantaneous streamline pattern, with two new semi-saddles (S_2', S_3') and a node (N). Dynamically, in Figs. 5(b)-5(d), we see that a set of fluid particles released right downstream trailing edge, although still turning around trailing edge and going upstream, have a tendency to lift up from the airfoil surface. This signifies the generic unsteady separation, or fluid-particle separation.[37,38]

Then, a critical event occurs at $t = 0.029$ ($Re(t) \approx 4554$), in which several qualitative changes take place:

(i) Associated with the quick growth of the sublayer with $\omega < 0$, the first semi-saddle S_1' runs to meet the new semi-saddle S_2' at upstream boundary of the bubble so that a new saddle S is formed in the streamline pattern (Fig. 5(d)), which rises up into the very narrow irrotational zone (green region in color). It satisfies the Moore-Rott-Sears (MRS) criterion,[39–41] and thus we identify S as an *instantaneous MRS point*, which marks the unsteady reattachment instead

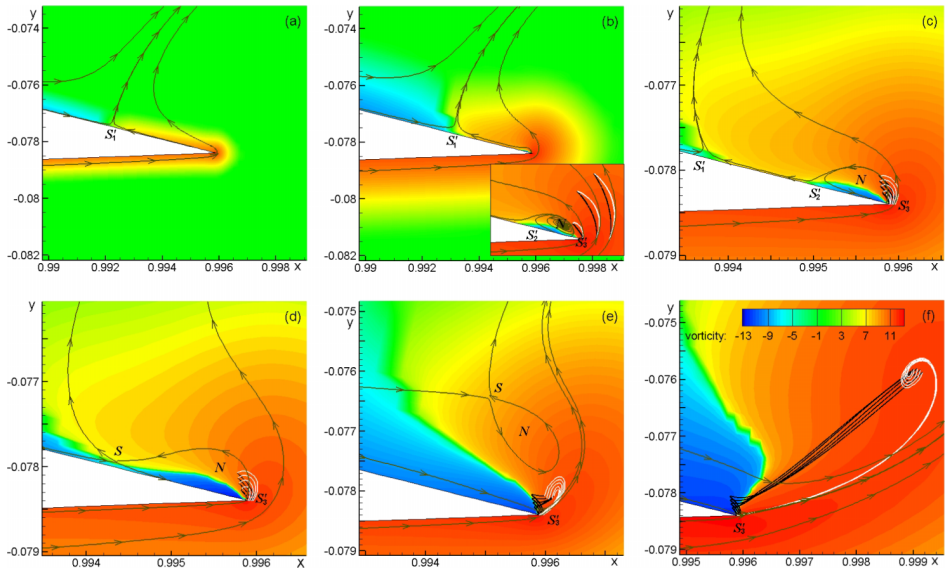

FIG. 5. Time variation of accelerated starting flow over NACA-0012 airfoil at $Re = 10^5$ when the flow becomes steady and $\alpha = 6°$: Contours of vorticity ω with color bar shown in (f), pathlines (black), streaklines (white), and streamlines (gray with arrows). Only the local flow field near trailing edge is shown. From (a) to (f): $t = 0.002, 0.02, 0.026, 0.029, 0.050, 0.100$. x, y are normalized by chord length of airfoil.

of separation, though. This MRS point has a very short life, since saddle S moves into vortical region for $t \geq 0.030$.

(ii) The bubble is lifted up that contacts the wall only at trailing edge, below which the two segments of shear layers of $\omega < 0$ merge to a single attached layer without separation. Thus, only a semi-saddle S_3' remains right at trailing edge, around which no more fluid particles can make turn. Instead, the lower-surface boundary layer with strong $\omega > 0$ has to shed from trailing edge into wake, becoming a *free shear layer*.

(iii) Those upstream-moving particles near trailing edge are blocked by the strong BVF and start to make sharp turns back toward downstream and are strongly lifted up. This is more clearly shown in Fig. 5(e) at $Re(t) \approx 7850$. Kinematically, the bubble described by the saddle-node pair of streamlines has been fully ejected from trailing edge into the flow field, which then quickly disappears (at about $t = 0.07$). Dynamically, on the one hand, in boundary-layer approximation, this sharp turn could be the signal of the singularity mentioned by Van Dommenlen and Shen,[42] where a packet of fluid particles stops their forward advance along the wall, and on the other hand, these particles' trajectories could be identified as the spikes of generic unsteady separation like in Haller's theory. This implies that the earlier generic separation at trailing edge, shown in Figs. 5(b)–5(d), has evolved to strong *unsteady boundary-layer separation* from trailing edge. But unlike generic separation where the spikes have a single envelope, as boundary-layer separation these particles would have a bundle of envelopes ejected into the wake. These particles carry positive vorticity and are immediately entrained by the strong free shear layer of $\omega > 0$ from lower side of trailing edge, as clearly seen from the streakline pattern.

(iv) As the shear layer carries vorticity into wake, the airfoil starts to gain a circulation $\Gamma(t) < 0$ (see Fig. 6). Slightly later, the layer quickly rolls into a concentrated axial vortex, namely, the *starting vortex*, and continuously feeds $\omega > 0$ into the vortex to keep its growth.

The starting vortex is well shaped at $t = 0.100$ (Fig. 5(f)). At this time, the streaklines and streamlines tend to leave the lower surface tangentially. But the pathlines do not (remember that their behavior near trailing edge is represented by snapshots at earlier times and now the same set of particles meet the latest end of streaklines).

As the incoming flow ceases to accelerate at $t = 1.0$, the flow gradually becomes fully attached and quasi-steady (not shown). The time-history of airfoil circulation up to $t = 1.0$ is shown in Fig. 6.

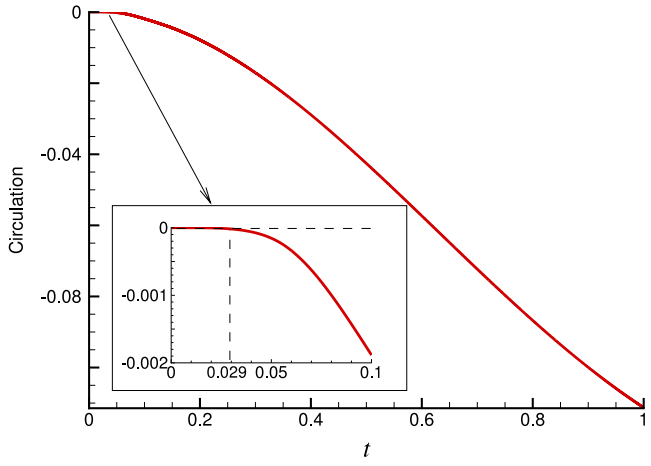

FIG. 6. Time history of airfoil circulation (including the circulation in attached bubble seen in Figs. 5(b) and 5(c)) up to $t = 1.0$.

After a certain time, the laminar wake at $Re = 10^5$ becomes unstable and the Γ-curve starts to oscillate. Its mean value approaches -0.32 at $t = 30$, in consistency with the classic thin airfoil theory where Γ approaches $-\pi\alpha \approx -0.329$ as $t \to \infty$.

D. Formation of circulation: Causal mechanisms

To understand the underlying causal mechanisms of the flow patterns in Fig. 5, we use vorticity formulation and show in Fig. 7 the on-wall distributions of dynamic quantities, including on-wall normal pressure gradient $\partial_n p$ given by (2b), boundary vorticity ω_B, boundary vorticity flux $\sigma = \partial_s p$, and boundary enstrophy flux $\eta \equiv \boldsymbol{\omega}_B \cdot \boldsymbol{\sigma}$ at selected times. These on-wall dynamic mechanisms exist for both steady and unsteady flows.

The initial flow pattern at $t = 0.002$ is associated with an inviscid effect and a viscous effect. The former is a very strong suction peak at TE (Fig. 7(a)) due to Equation (2b), of which the magnitude decreases monotonically with time. The latter is a thin attached boundary layer with no circulation, having $\omega < 0$ (clockwise) upstream S_1', and $\omega > 0$ downstream S_1' on upper surface and over the lower surface (Figs. 5(a) and 7(b)).

In terms of vorticity formulation, the key observation is that the high-p at S_1' and low-p at trailing edge imply a pair of BVF peaks at both sides near trailing edge (Fig. 7(c)), which at $t = 0.002$ are quite weak due to relatively small $Re(t) \approx 314$, but soon become extremely strong. Here, the dynamic (σ,ω)-coupling dominates the later flow evolution. Specifically, the key causal mechanisms of this coupling are the formation of pressure distribution over airfoil surface and its tangent gradient as predicted by potential-flow theory; BVF (namely, tangent pressure gradient) creates new vorticity via no-slip condition; vorticity is diffused into the fluid and advected downstream, which in turn alters existing ω in the flow field. Note that these and all events of vorticity evolution analyzed below are associated with a varying velocity field via the Biot–Savart formula, which is a kinematic rather than causal relation.

At $t = 0.020$ ($Re(t) \approx 3140$), typical high-Re viscous flow behavior starts to show up. The BVF peaks near trailing edge have grown to be very strong (Fig. 7(c)). The big positive BVF peak at lower surface enhances the existing $\omega > 0$ to form a strongly attached boundary layer there. The big negative BVF peak at upper surface generates new $\omega < 0$ and diffuses it into the fluid to weaken the existing $\omega > 0$ downstream S_1' (Fig. 5(b)) and even alter the sign of ω_B, resulting in separation. This latter event is also marked by the boundary enstrophy flux η crossing zero (see point A of Figs. 7(b) and 7(d)). In addition, the normal pressure gradient is significantly reduced (Fig. 7(a)), since the bubble smoothes out the trajectory of fluid particles turning around trailing edge (see Fig. 5(b)).

Remarkably, the BVF peaks remain strong for $t \in (0.020, 0.100)$ (Fig. 7(c)). In particular, within $\Delta t = 0.01$, the negative BVF peak on upper surface causes the bubble to be quickly and strongly

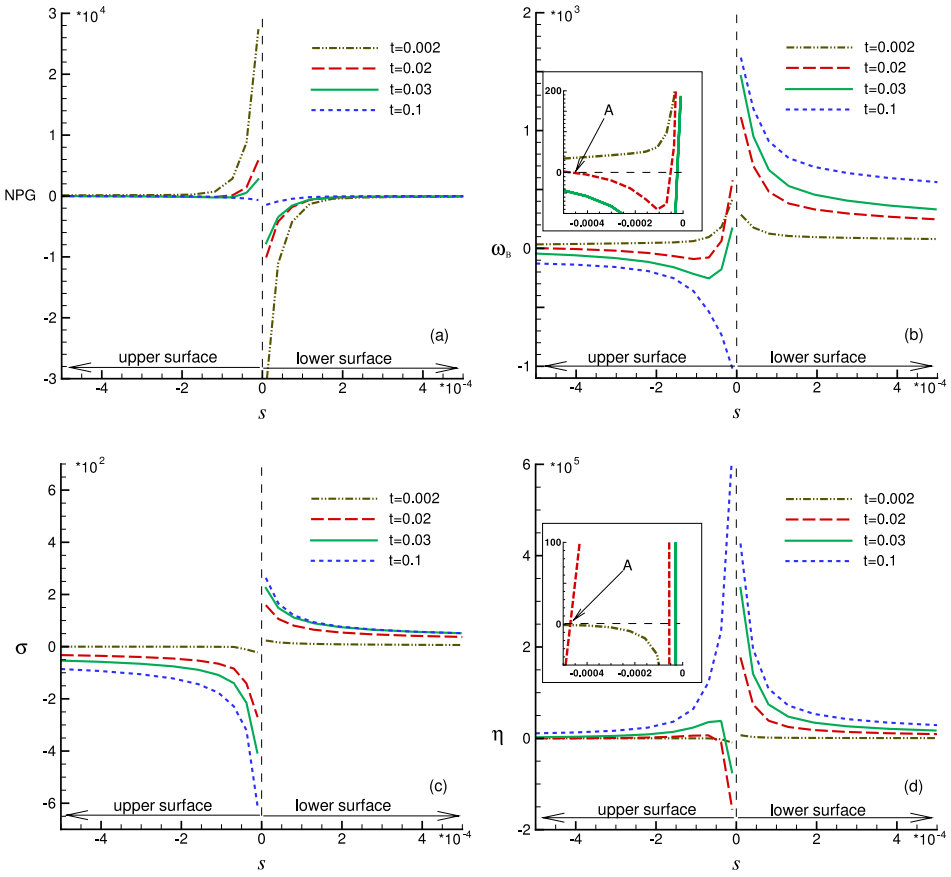

FIG. 7. Distributions of boundary quantities: (a) normal pressure gradient (NPG), (b) on-wall vorticity (ω_B), (c) boundary vorticity flux (σ), and (d) boundary enstrophy flux (η) at selected times. Curves of ω_B and η cross zero at point A and $t = 0.020$, anticipating fluid-particle separation. For the definition of coordinate s see the caption of Figure 4.

enlarged in both thickness and length (see Fig. 5(c)), which accelerates the downstream motion of the semi-saddle S_1'. Such distributions of σ and η imply that separation is inevitable.

At $t = 0.100$, both the trailing-edge suction peak and strong BVF peaks nearby start to decrease, and all the peaks of normal pressure gradient, boundary vorticity flux, and boundary enstrophy flux near trailing edge disappear at $t = 1.0$. Finally, the flow becomes quasi-steady and no more net vorticity is fed into the starting vortex.

IV. REALIZATION OF KUTTA CONDITION

The Kutta condition was originally introduced as an empirical artifact to eliminate the indeterminacy of circulation for two-dimensional doubly connected potential flow over the airfoil, by requiring the regularity of the flow at sharp trailing edge. But it has long been recognized that the condition is a natural result of viscous flow. The effects of complicated viscous processes that lead to the circulation "are summed up, approximately, in the Kutta-Joukowski trailing-edge condition."[41] It also exists in three-dimensional wing flow although the flow domain is singly connected.[43] While the Kutta condition is no longer needed in viscous-flow theory, it is of interest to examine how the flow status stated by the condition is naturally realized or approximately satisfied.

The Kutta condition has been stated in various ways by different authors, which in viscous flow corresponds to certain specific events. Below we list a few.

1. G-event: *"the flow must leave the trailing edge smoothly,"* stated by Glauert[8] (p. 119); see also Thwaites[44] (p. 179).

2. KB-event: *"in the final steady flow, the rear stagnation point shall coincide with the trailing edge of the airfoil,"* stated by von Kármán and Burgers[9] (p. 13); see also Batchelor[11] (p. 437).
3. T-event: *"the total flux of vorticity into the wake must be zero for steady flow,"* stated by Taylor.[7]
4. S-event: *"the pressures at the trailing edge shall have the same value when determined from the potential-flow values above and below the airfoil,"* proposed by Spence[45] and stated by Sears.[41]

Sears[41] has proven that the T-event and S-event are equivalent for incompressible viscous flows. We state them separately because this equivalence is no longer true for supersonic flow, where only S-event holds for flow downstream of trailing-edge shocks.

It is well known that the Kutta condition must be satisfied when the flow finally becomes steady. Indeed, in steady incompressible flow, the G-event, KB-event, T-event, and S-event merge to one. However, referring to Fig. 5, obviously the Kutta condition is not realized immediately after the flow starts. Instead, the most remarkable finding is that all these events have been confirmed to appear in the *unsteady* viscous transient flow, but they take place one after another.

First, the KB-event occurs at $t = 0.029$, when there starts to remain only a single semi-saddle at trailing edge on the rear portion of airfoil surface. According to our preceding discussion, we see that the KB-version of the Kutta condition captures precisely the moment when the airfoil starts to gain circulation. Next, the G-event occurs at $t \approx 0.10$, when the separated shear layer starts to leave the lower surface at trailing edge smoothly. Finally, the T-event and S-event do not take place till much later, at $t > 1.0$, when both normal pressure gradient and boundary vorticity flux vanish at trailing edge and the flow becomes asymptotically steady.

The sequential appearance of different "Kutta events" in unsteady transient flow is of interest in unsteady aerodynamics, for example, flapping-wing flow in animal flight. In the past, the Kutta condition for unsteady flow has been studied in the context of both aerodynamics as reviewed by Bassanini *et al*.,[43] and interaction of acoustic wave and shear flow at sharp edges as reviewed by Crighton.[46] Now, for unsteady flow over a body with sharp edge, most of the theoretical models and numerical schemes do not have sufficient accuracy to capture the details of critical events near trailing edge. They still have to appeal to certain Kutta condition even in viscous flow, similar to the equal-pressure or equal-vorticity flux condition for steady flow. In this case, it would be important to choose a proper condition among different versions, and to decide whether it should be imposed all the time or only in part time. This issue deserves further investigation but is beyond the concern of the present paper.

V. CONCLUSIONS

1. The lift is generated by a wing through a chain of complex processes. Identifying this physical chain is far more involved than deriving lift formulas themselves, even in the simplest case of two-dimensional incompressible flow over an airfoil. Once Kutta-Joukowski formula (1) was established and then airfoil's circulation was found to be carried by airfoil's boundary layer in viscous flow, a key issue of tracing the origin of lift is naturally focused on the causal mechanisms of vorticity creation at airfoil surface. These mechanisms can be clearly revealed in terms of vorticity formulation and are of general significance in practical wing design and flow control.
2. The whole scenario of the formation of airfoil circulation has been went through by Navier-Stokes numerical simulation for two-dimensional incompressible starting flow past an airfoil. Clear and detailed interpretation of the flow development is given in terms of vorticity formulation, in which causal relation of tangent pressure gradient and BVF plays a central role. Specifically, the circulation-formation process can be summarized as follows:

   - As an incoming viscous fluid starts to move at $t = 0$ over a stationary airfoil, either impulsively or through a finite transient acceleration, the first causal mechanism is the formation of pressure distribution over airfoil surface and its tangent pressure gradient as predicted by potential-flow theory. But by no-slip condition, tangent pressure gradient causes BVF almost immediately, and the inviscid initial slip velocity over the airfoil becomes a distributed vortex sheet. In this stage, the airfoil has no circulation, with a very rapid fluid motion around the sharp TE from lower to upper surface, associated with an extremely low suction peak and an almost singular tangent pressure gradient near trailing edge.

- The singular tangent pressure gradient implies a pair of sharp BVF peaks that create new vorticities at both sides of the airfoil near trailing edge after $t = 0$. Meanwhile, the vortex sheet evolves to thin boundary layers by diffusion. At the lower surface, the positive BVF peak enhances the existing positive boundary-layer vorticity, making the layer tightly attached with stronger shear. But at the upper surface the negative BVF peak counteracts the existing positive boundary-layer vorticity downstream the rear semi-saddle, leading to a separated bubble upstream trailing edge with recirculating flow therein, which may remain attached in a short time. This event signifies unsteady fluid-particle separation.
- Still due to the strong BVF peak at upper surface near trailing edge, the upstream moving fluid particles round trailing edge are blocked and turn sharply into the main stream. This event signifies the separation of whole boundary layer from trailing edge. At this moment, the bubble detaches from the wall, forming an instantaneous MRS point, the rear stagnation point sits at trailing edge, and the entire upper-surface boundary layer of negative vorticity starts to be fully attached. This event is what described by von Kármán and Burgers[9] as the marker of Kutta condition, but in unsteady flow. Meanwhile, the sharply turning fluid packet starts to meet the strong lower boundary layer at trailing edge, forming a free shear layer which carries some positive circulation away from the airfoil. Thus, the airfoil starts to gain a negative circulation.
- At a later time, the separated shear layer tends to leave trailing edge in tangent direction and rolls into a concentrated starting vortex. The vortex is continuously enhanced by vorticity feeding in from the free shear layer. This event is what described by Glauert[8] as the marker of Kutta condition, but again in unsteady flow. At an even later time, the peaks of normal pressure gradient and BVF at trailing edge disappear, the total vorticity advection flux into the wake reduces to zero, and the pressures at upper and lower surfaces become equal. The feeding sheet of starting vortex is cut off. This event is what described by Taylor,[7] Spence,[45] and Sears[41] as the marker of Kutta condition, but still in unsteady flow. Since then the flow develops smoothly to steady state with a constant airfoil circulation.

The unsteady Kutta condition in general viscous flow is still an open problem and deserves further investigation. In addition, the analysis method we adopted in our present study may be extended to flexible-wing flow, which is a very active research field currently.

ACKNOWLEDGMENTS

This work was supported in part by NSFC (Grant Nos. 11221062 and 11472016) and MOST of China (Grant No. 2009CB724100). We are very grateful to Dr. Fanglin Zhu for permitting us to use his code. We also thank Professor Wei-Dong Su, Professor Yi-Peng Shi, and Professor Feng Liu, and Mr. An-Kang Gao for very valuable comments. In particular, we thank very much a referee who called our attention to the important effect of different starting-flow modes on the formation process of airfoil circulation, as addressed in Section III A.

[1] W. Kutta, "Lift forces in flowing fluids," Aeronaut. Mitt. **III**, 133–135 (1902).
[2] N. Jowkowski, "De la chute dans I'air de corps légers de forme allongée, animés d'un mouvement rotatoire," in *Bulletin de I'Institute Aérodynamic de Koutchino* (Fascicule 1, St. Petersburg, 1906).
[3] O. Darrigol, *Worlds of Flow* (Oxford University Press, 2005).
[4] D. Bloor, *The Enigma of the Aerofoil* (University of Chicago Press, 2011).
[5] T. S. Liu, J. Z. Wu, J. Y. Zhu, S. F. Zou, and L. Q. Liu, "The origin of lift revisited: I. A complete theory," AIAA Paper 2015–2302 2015.
[6] L. W. Bryant, D. H. Williams, and G. I. Taylor, "An investigation of the flow of air around an aerofoil of infinite span," Philos. Trans. R. Soc., A **225**, 199 (1926).
[7] G. I. Taylor, "Note on the connection between the lift in an airfoil in a wind and the circulation round it," Philos. Trans. R. Soc., A **225**, 238 (1926).
[8] H. Glauert, *The Elements of Aerofoil and Airscrew Theory* (Cambridge University Press, 1926).
[9] Th. von Kármán and J. M. Burgers, "General aerodynamic theory—Perfect fluids," in *Aerodynamic Theory*, edited by W. F. Durand (Springer, 1935), Vol. II, pp. 1–24.
[10] L. Prandtl and O. G. Tietjens, *Fundamentals of Hydro and Aerodynamics* (Dover, 1934).
[11] G. K. Batchelor, *An Introduction to Fluid Dynamics* (Cambridge University Press, 1967).
[12] H. J. Lugt and H. J. Haussling, "Laminar flow past an abruptly accelerated elliptic cylinder at 45° incidence," J. Fluid Mech. **65**, 711 (1974).

[13] U. B. Mehta and Z. Lavan, "Starting vortex, separation bubbles and stall: A numerical study of laminar unsteady flow around an airfoil," J. Fluid Mech. **67**, 227 (1975).
[14] C. C. Chang, Y. C. Hsiau, and C. C. Chu, "Starting vortex and lift on an airfoil," Phys. Fluids A **5**, 2826 (1993).
[15] H. J. Lugt, *Vortex Flow in Nature and Technology* (Krieger Publishing Company, 1995).
[16] F. T. Muijres, L. C. Johansson, R. Barfield, M. Wolf, G. R. Spedding, and A. Hedenström, "Leading-edge vortex improves lift in slow-flying bats," Science **319**, 1250 (2008).
[17] C. W. P. Ford and H. Babinsky, "Lift and the leading-edge vortex," J. Fluid Mech. **720**, 280 (2013).
[18] D. Tam, "Flexibility increases lift for passive fluttering wings," J. Fluid Mech. **765**, R2 (2015).
[19] D. McLean, *Understanding Aerodynamics* (Wiley, 2012).
[20] M. J. Lighthill, "Introduction: Boundary layer theory," in *Laminar Boundary Layers*, edited by L. Rosenhead (Clarendon Press, 1963), pp. 46–113.
[21] J. Z. Wu, H. Y. Ma, and M. D. Zhou, *Vorticity and Vortex Dynamics* (Springer, 2006).
[22] J. Z. Wu, H. Wu, and Q. S. Li, "Boundary vorticity flux and engineering flow management," Adv. Appl. Math. Mech. **1**, 353 (2009).
[23] J. Y. Zhu, F. L. Zhu, W. D. Su, S. F. Zou, L. Q. Liu, Y. P. Shi, and J. Z. Wu, "A vorticity dynamics view of 'effective slip boundary' with application to foil-flow control," Phys. Fluids **12**, 123602 (2014).
[24] M. J. Lighthill, "Viscosity effects in sound waves of finite amplitude," in *Surveys in Mechanics*, edited by G. K. Batchelor and R. M. Davies (Cambridge University Press, 1956), pp. 250–351.
[25] H. Schlichting and K. Gersten, *Boundary Layer Theory* (Springer, 2000).
[26] C. Truesdell, *The Kinematics of Vorticity* (Indiana University Press, 1954).
[27] J. C. Wu, "Numerical boundary conditions for viscous flow problems," AIAA J. **14**, 1042 (1976).
[28] T. J. Chung, *Computational Fluid Dynamics* (Cambridge University Press, 2002).
[29] J. Z. Wu, X. H. Wu, H. Y. Ma, and J. M. Wu, "Dynamic vorticity condition: Theoretical analysis and numerical implementation," Int. J. Numer. Methods Fluids **19**, 905 (1994).
[30] S. C. Huang and R. B. Kinney, "Unsteady viscous flow over a grooved wall: A comparison of two numerical methods," Int. J. Numer. Methods Fluids **8**, 1403 (1988).
[31] P. Koumoutsakos, A. Leonard, and F. Pepin, "Boundary conditions for viscous vortex methods," J. Comput. Phys. **113**, 52 (1994).
[32] P. Koumoutsakos and A. Leonard, "High-resolution simulations of the flow around an impulsively started cylinder using vortex methods," J. Fluid Mech. **296**, 1 (1995).
[33] F. L. Zhu, "Applications of boundary vorticity dynamics in flow simulation, airfoil design, and flow control," Ph.D. dissertation (University of Tennessee, 2000).
[34] M. Kurosaka and P. Sundaram, "Illustrative examples of streaklines in unsteady vortices: Interpretational difficulties revisited," Phys. Fluids A **29**, 3474 (1986).
[35] P. Sundaram, M. Kurosaka, and J. M. Wu, "Vortex dynamics analysis of unsteady vortex wakes," AIAA J. **29**, 321 (1991).
[36] A. E. Perry, M. S. Chong, and T. T. Lim, "The vortex-shedding process behind two-dimensional bluff bodies," J. Fluid Mech. **116**, 77 (1982).
[37] G. Haller, "Exact theory of unsteady separation for two-dimensional flows," J. Fluid Mech. **512**, 257 (2004).
[38] A. Surana, G. B. Jacobs, O. Grunberg, and G. Haller, "An exact theory of three-dimensional fixed separation in unsteady flows," Phys. Fluids **20**, 107101 (2008).
[39] F. K. Moore, "On the separation of unsteady boundary layer," in *Boundary-Layer Research*, edited by H. Gortler (Springer, 1958), pp. 296–311.
[40] N. Rott, "Unsteady viscous flows in the vicinity of a separation point," Q. Appl. Math. **13**, 444 (1956).
[41] W. R. Sears, "Some recent developments in airfoil theory," J. Aeronaut. Sci. **23**, 490 (1956).
[42] L. L. Van Dommenlen and S. F. Shen, "The genesis of separation," in *Numerical and Physical Aspects of Aerodynamic Flows*, edited by T. Cebeci (Springer, 1982), pp. 293–311.
[43] P. Bassanini, C. M. Casciola, M. R. Lancia, and R. Piva, "Edge singularities and Kutta condition in 3D aerodynamics," Meccanica **34**, 199 (1999).
[44] *Incompressible Aerodynamics*, edited by B. Thwaites (Clarendon Press, 1960).
[45] D. A. Spence, "Prediction of the characteristics of two-dimensional airfoil," J. Aeronaut. Sci. **21**, 577 (1954).
[46] D. G. Crighton, "The Kutta condition in unsteady flow," Annu. Rev. Fluid Mech. **17**, 411 (1985).